



# MIT Open Access Articles

## *Real-Time Physiological Measurement and Visualization Using a Synchronized Multi-camera System*

The MIT Faculty has made this article openly available. **Please share** how this access benefits you. Your story matters.

<b>Citation</b>	Gupta, Otkrist, McDuff, Daniel and Raskar, Ramesh. 2016. "Real-Time Physiological Measurement and Visualization Using a Synchronized Multi-camera System."
<b>As Published</b>	10.1109/CVPRW.2016.46
<b>Publisher</b>	Institute of Electrical and Electronics Engineers (IEEE)
<b>Version</b>	Author's final manuscript
<b>Citable link</b>	<a href="https://hdl.handle.net/1721.1/138100">https://hdl.handle.net/1721.1/138100</a>
<b>Terms of Use</b>	Creative Commons Attribution-Noncommercial-Share Alike
<b>Detailed Terms</b>	<a href="http://creativecommons.org/licenses/by-nc-sa/4.0/">http://creativecommons.org/licenses/by-nc-sa/4.0/</a>

# Real-Time Physiological Measurement and Visualization Using a Synchronized Multi-Camera System

Otkrist Gupta

otkrist@mit.edu

Daniel McDuff

djmcduff@mit.edu

Ramesh Raskar

Media Lab

Massachusetts Institute of Technology, Cambridge, MA, USA

raskar@media.mit.edu

## Abstract

*Remote physiological measurement has widespread implications in healthcare and affective computing. This paper presents an efficient system for remotely measuring heart rate and heart rate variability using multiple low-cost digital cameras in real-time. We combine an RGB camera, monochrome camera with color filter and a thermal camera to recover the blood volume pulse (BVP). We show that using multiple cameras in synchrony yields the most accurate recovery of the BVP signal. The RGB combination is not optimal. We show that the thermal camera improves performance of measurement under dynamic ambient lighting but the thermal camera alone is not enough and accuracy can be improved by adding more spectral channels. We present a real-time prototype that allows accurate physiological measurement combined with a novel user interface to visualize changes in heart rate and heart rate variability. Finally, we propose how this system might be used for applications such as patient monitoring.*

## 1. Introduction

Non-contact measurement of physiological parameters (such as heart rate and heart rate variability) has much potential for healthcare (e.g telemedicine) and affective computing applications. The inter-beat intervals (IBI) of the heart are influenced by both the sympathetic and parasympathetic branches of the autonomic nervous system (ANS) activity. Heart rate variability (HRV) is typically calculated by performing time domain and/or frequency domain analysis of the IBIs [1]. The HRV low frequency (LF) component is modulated by baroreflex activity and contains both sympathetic and parasympathetic activity. The high frequency (HF) component reflects parasympathetic influence on the

heart, it is connected to respiratory sinus arrhythmia (RSA). HRV can be used as a measure of stress (caused by physical activity, cognitive activity and/or emotions). Traditionally physiological measurement has been performed using dedicated contact sensors and sticky electrodes. These sensors can be expensive and uncomfortable to wear.

Photoplethysmography (PPG) is the process of measuring blood flow from light transmitted through, or reflected from, the skin [2]. PPG allows for unobtrusive recovery of the cardiac signals via the blood volume pulse (BVP). Typically BVP is measured using a custom sensor in contact with the skin and a dedicated light-source (such as a light emitting diode (LED)). Recently, it has been shown that remote physiological measurement can be performed using ambient light and digital cameras [23]. Heart rate, breathing rate and heart rate variability can all be measured using this approach [17, 18]. Preliminary results on the measurement of blood oxygenation have also been shown [20]. In previous work the green color channel from the camera was found to have the strongest signal from the three RGB color channels. However, the RGB channel combination is not optimal for this problem and such techniques can fail under illumination variation. McDuff *et al.* [14] showed that other color bands (cyan and orange) yielded more accurate results. In this work we use a flexible camera array and capture multiple spectra by combing color filters on commercially available monochrome cameras.

Most remote PPG measurement methods involve capturing the color changes across a region of skin (typically on the face) by spatially averaging pixel values, forming temporal color channel signals and applying a combination of source separation and filtering steps to recover the BVP. There still remain a number of open questions with respect to optimizing this approach [13]. The impact of motion of the subject and changes in illumination are two important factors that would influence a practical system. Estep *et*

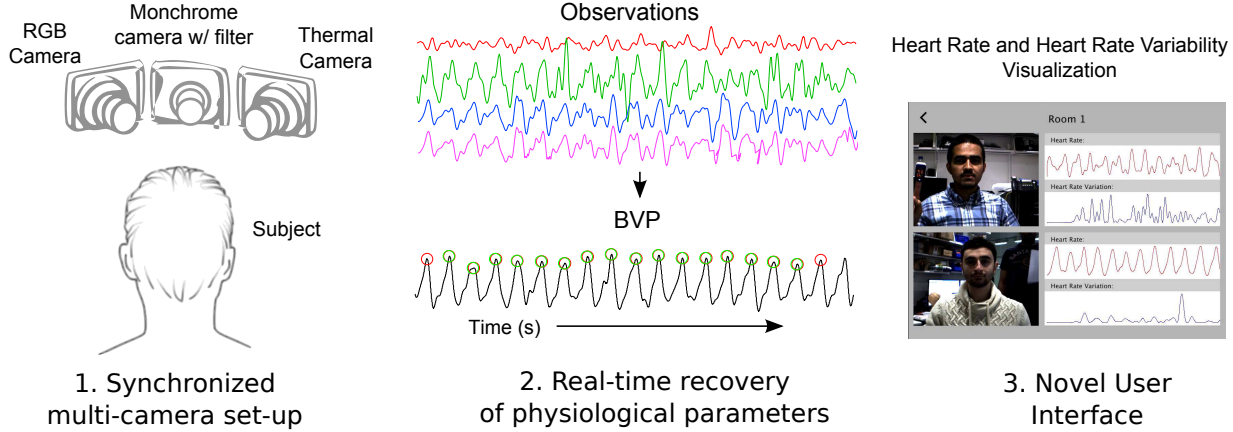


Figure 1. We present a novel system for real-time physiological measurement and visualization. 1) A synchronized multi-camera apparatus including an RGB camera, a monochrome camera with color filter and a thermal camera. 2) Real-time recovery of blood volume pulse, heart rate and heart rate variability. 3) A novel user interface for visualizing heart rate and heart rate variability.

*al.* [8] use a multi-imager array for remote pulse rate measurement and show that the increased number of observations can improve the accuracy in the presence of head motions. A hybrid approach using a visual spectrum and thermal camera for measuring physiological parameters from the hand was presented by Blanik *et al.* [4]. However, this was not a low-cost solution due to the thermal camera used.

Cardiovascular parameters (particularly HRV) can be useful in predicting cognitive load [15, 16]. Bousefsaf *et al.* [5] showed that remotely measured physiological parameters can be used to capture changes in workload when participants completed a Stroop task. However, in neither case was this performed in real-time or with information from more than one camera. The experiments until now have relied mostly on visible spectrum light and off-line processing. We show that a multi-spectral and thermal approach can improve measurements, especially in the presence of illumination changes. Furthermore, we present a real-time implementation and novel visualization of the data. Figure 1 shows a high-level overview of our approach. Table 1 presents a comparison of our work against others.

### 1.1. Contributions

To our knowledge this is the first work to propose a real-time system using a thermal camera with multi-spectral imaging to deduce heart rate under illumination variation. The main contributions of this paper are to present:

1. A novel **multi-camera** setup to capture physiological measurements using **multi-spectral** techniques.
2. A low-cost **real-time** system that can accurately capture heart rate and HRV measurements.
3. A demonstration of how to combine a **thermal camera** with multi-spectral camera(s) to further improve

Paper	Multi-Cam	Multi-Spectral	Illum. Invari.	Real-Time
Poh <i>et al.</i> [17, 18]	✗	✗	✗	✗
Estep <i>et al.</i> [8]	✓	✗	✗	✗
Blanik <i>et al.</i> [4]	✓	✗	✗	✗
McDuff <i>et al.</i> [14]	✗	✓	✗	✗
<b>Our Paper</b>	✓	✓	✓	✓

Table 1. Our paper proposes a multi-camera, multi-spectral, real-time system for measuring and visualizing physiological responses robustly under illumination variation.

performance and potentially present a more robust approach under dynamic ambient light.

4. A technique for **visualizing changes in stress** (linked to autonomic nervous system activation) and heart rate in real-time. A user interface to show vital signs of multiple patients in a hospital using the data captured from the cameras.

## 2. Related Works

The remote measurement of physiological parameters has been demonstrated using laser Doppler [22], microwave Doppler [7] and thermal cameras [9]. Recently, it has been shown that the blood volume pulse can be recovered using visible light and a digital camera [23]. Furthermore, this can be performed using a low-cost webcam [17]. Accurate measurement of heart rate, respiration rate and heart rate variability parameters is possible for stationary individuals under stable ambient lighting [18]. The sensitivity of the camera sensor was not explored. In subsequent work the red, green and blue (RGB) color bands were found to not be the optimal combination. McDuff *et al.* [14] tested five color bands, RGB, cyan and orange. The combination of cyan,

green and orange was found to outperform RGB. The color sensitivity of the sensor was not further optimized. Motion and dynamic illumination can impact the performance of remote physiological measurement using ambient light and a digital camera. A number of approaches have been presented to help mediate the performance impact. Sun *et al.* [19] presented a method for motion-compensation accounting for planar motion.

Tarassenko *et al.* [20] presented initial results of oxygen saturation measurements from a digital camera in a clinical study. Population-based calibration was required to fix two parameters. Balakrishnan *et al.* [3] showed that the human pulse could be captured from subtle head motions. However, this approach is very sensitive to gross head motions. Wu *et al.* presented a novel method to amplify the PPG signal in videos using Eulerian magnification [24]. However, this approach does not provide a way of finding the pulse frequency automatically.

### 3. Approach

Figure 2 provides an overview of our approach. Our setup takes synchronized video of a person’s face through a combination of: a color (RGB) camera, a monochrome camera and a thermal sensor array. We apply a filter at the aperture of the monochrome camera to capture images from another color channel. In this analysis we used a magenta filter. However, the filter could be optimized for the specific application considered. The video is processed in an uncompressed raw format to prevent signal loss due to video compression (the BVP measurement involves picking up sub-pixel level variations in color channel signals). We first localize the face and facial features, using the facial segmentation described below, and define a region of interest (ROI) on the face. We aggregate the camera channel values for each frame and represent each as a time varying series  $x_n(t)$ , where  $n$  represents the channel. The ROI ignores pixels around the eyes and mouth to prevent noise from blinking and speaking. We capture the raw readout from the 8x8 thermal sensor array connected to computer in parallel with the RGB camera using a separate thread.

For comparison with the current gold-standard in BVP measurement we simultaneously capture a raw PPG signal from a contact finger PPG sensor on the index finger of the participant.

#### 3.1. Facial Segmentation

We use conditional regression forests (CRF) [6] to perform facial landmark detection in real-time. The lip corners, lip top and bottom, and outer eye corners are used to isolate the region of interest (ROI). Real-time tracking of facial features allows us to accommodate subject head motions and mitigate small changes in face orientation. We select the ROI from the cheeks and forehead as these re-

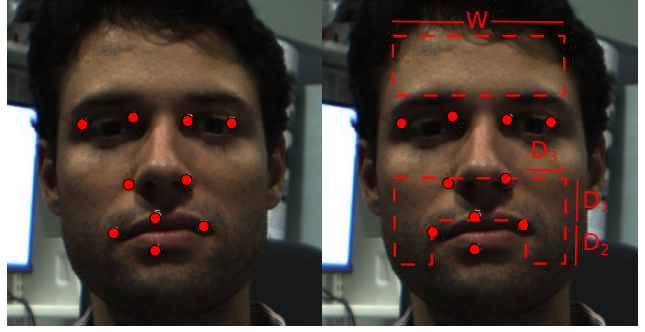


Figure 3. Left) Facial landmark points identified on the face. Right) The facial region of interest (ROI) used for calculating the BVP signal.  $W$ ,  $D_1$ ,  $D_2$ , and  $D_3$  are defined in Section 3.1.

gions of the face have been shown to contain the strongest PPG signal [12]. As shown in Figure 3, we set the width of the ROI ( $W$ ) equal to the distance between outer eye corners. We set the height of the forehead ROI to be one third of the distance between eye corners ( $W/3$ ). We leave margins ( $W/4$ ) above and below the eye corners for both the forehead and nose ROIs. The nose ROI height ( $D_1$ ) is selected from the nose tip to the lip top. The cheek ROIs extend from extreme eye corners to lip corners ( $D_3$ ). The height of the cheek ( $D_1 + D_2$ ) ROI is measured from the nose tip to the bottom lip. We extend the ROI selection to multiple cameras by applying the same facial segmentation algorithms described above. To optimize for camera arrays with cameras placed at small offset  $x$ , we calculate the offset  $x$  in the image features from the landmark points and apply that to offset the bounding boxes. See Section 4 for detailed discussion on how the cameras were synchronized to acquire frames. These dimensions were not optimized but were found to yield good results.

#### 3.2. Signal Acquisition

Once we have acquired the ROI for each camera we calculate the spatial average of the pixel values within the ROI for each camera channel (RGBMT). The signal acquired for each spectral range can be represented as a time varying signal  $x_n(t)$  where  $n$  is number of spectral groups and  $t$  is the timestamp of each individual frame. The signal acquired can have sudden jumps due to variation in illumination conditions, which can be removed by taking a derivative and thresholding the values above 99% of one standard deviation and reintegrating. This removes any high frequency noise (for example, due to someone switching on a light in the room). We remove very low frequency trends in the signal by applying a detrending approach discussed in [21]. We can model the blood volume pulse signal being conveyed in the observed spectral channels as a blind source separation (BSS) problem. The BSS problem is modeled as a linear system as given below:



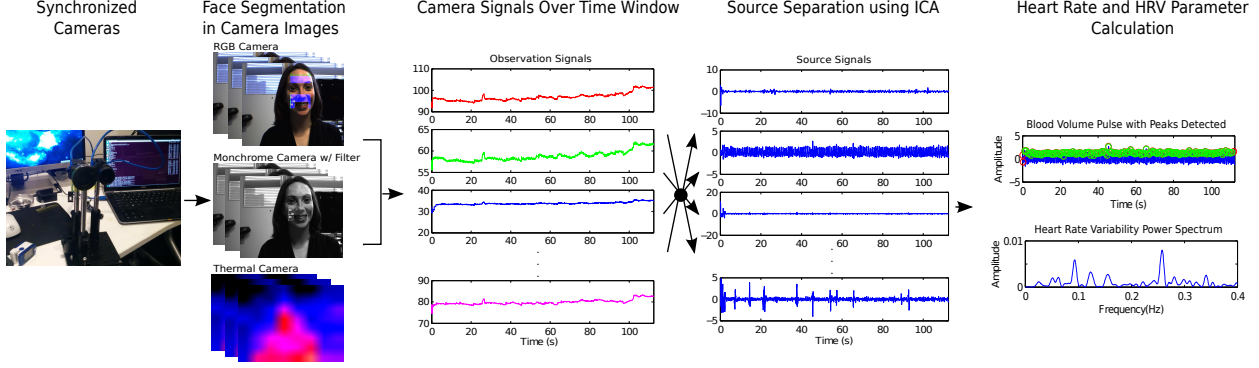


Figure 2. Overview of the remote physiological parameter estimation. 1) Multiple synchronized cameras are used to capture simultaneous video streams. 2) The face region of interest (ROI) within the video streams is detected and a spatial average of the pixels taken for each channel (red, green, blue, magenta, thermal). 3) Spatial time series signals are collected over a window. 4) ICA is used to recover the underlying source signals and the selected source bandpass filtered. 5) Peak detection is performed on the selected BVP. Heart rate and heart rate variability parameters are calculated. Calculations are performed with a moving window to continuously update estimations.

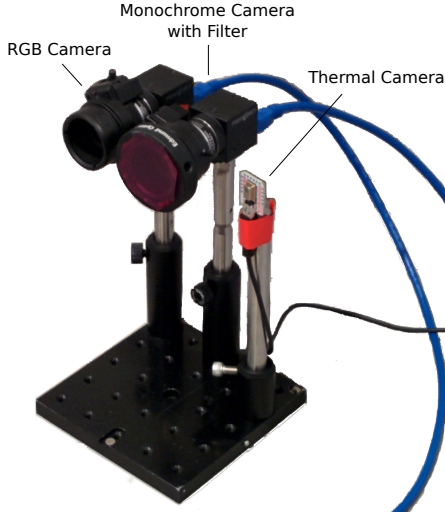


Figure 4. The multi-camera set-up used in our experiments. We combine an RGB camera, a monochrome camera with color filter and a thermal camera. The combination of multiple observations yields the best results, especially under dynamic illumination.

$$\mathbf{x}(t) = A\mathbf{s}(t) \quad (1)$$

Here  $A$  is an unknown mixing matrix,  $x(t)$  is the observed spectral channel and  $s(t)$  are the sources responsible for observations. One of the sources originates from light reflected back to camera after subsurface scattering. Oxygenated blood has a different light absorption coefficient at different frequencies compared to de-oxygenated blood which leads to periodic variation in intensity of scattered light. Transmitted light ( $I$ ) is linked to the concentration of oxygen in the blood ( $\Sigma$ ) and the light path length ( $l$ ) as given by the Beer-Lambert law:

$$T = \frac{I}{I_o} = e^{-\Sigma l} \quad (2)$$

There are many ways to solve  $s(t)$  but they all rely on making assumptions about sources and estimating the demixing matrix  $W \approx A^{-1}$ . In ICA we assume that all sources are independent and compute the demixing matrix which maximizes the non-gaussianity of sources. We use the Fast ICA algorithm [10] to run blind source separation. We choose to use Fast ICA, rather than the JADE based implementation, because it provides similar quality results at much faster speeds. While conventional algorithms rely on *kurtosis* or 4th order moment ( $E\{s(t)^4\} - 3 * (E\{s(t)^2\})^2$ ) as a measure of non-gaussianity, Fast ICA uses *negentropy* and maximizes that for the sources using the following fixed point algorithm (simplified for a one source case):

---

**Algorithm 1** Generating the demixing vector  $w$ .

---

```

 $f(z) \leftarrow \tanh(z)$ 
 $g(z) \leftarrow ue^{-u^2/2}$ 
 $w \leftarrow \text{random}(t)$ 
while !converged do
     $w^+ \leftarrow E(x f(w^T x)) - E(g(w^T x))w$ 
     $w \leftarrow (w^+) / (\|w^+\|)$ 
end while

```

---

We apply a bandpass filter with low and high frequency cut-offs at 0.8 and 2.2 Hz respectively to remove noise. The source signal with the greatest frequency power component between 0.8 and 2.2 Hz is selected as the BVP signal. The cut-off frequencies are chosen as reasonable upper and lower bounds for human heart rates. In our real-time demo we ran ICA over 2 minute windows (approximately 2500 frames) of  $x_n(t)$ . Since FastICA computation time can vary we run it in a separate thread every 5 seconds (110

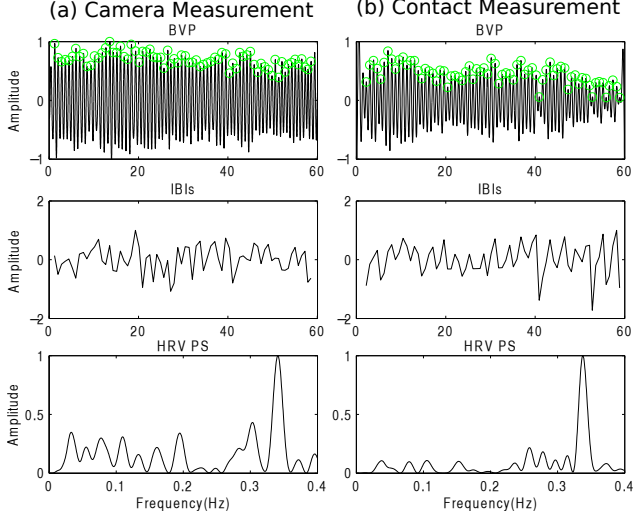


Figure 5. Calculation of the HRV spectrum from the BVP signal. Left) Camera measurements. Right) Contact measurements. Top) BVP signal recovered from cameras. Middle) Inter-beat intervals (IBIs) calculated from the BVP signal. Bottom) Heart rate variability spectrum calculated from the IBIs. Our HRV measure that is visualized is the ratio of the normalized low (0.04-0.15Hz) and high (0.15-0.4Hz) frequency powers.

frames) and display the PPG waveform of the person offset by 5 seconds.

### 3.3. Signal Analysis

Sources computed using ICA suffer from two inherent ambiguities: (1) Permutation ambiguity and (2) Scale and magnitude ambiguity as explained by following equations:

$$\mathbf{x} = \mathbf{A}\mathbf{s} = \mathbf{A}\mathbf{P}^{-1}\mathbf{P}\mathbf{s} = \mathbf{A}'\mathbf{s}' \quad (3)$$

$$\mathbf{x} = \mathbf{A}\mathbf{s} = \sum_{j=1}^n a_j s_j = \sum_{j=1}^n (a_j / \alpha_j) (\alpha_j s_j) = \mathbf{A}'\mathbf{s}' \quad (4)$$

We use the technique adopted by Poh *et al.* [17] and select the source by normalizing the FFT of each source and selecting the source with highest peak ( $\arg \max\{\max(FFT\{s_n(t)\})\}$ ). To rectify any flipped signals (caused by scaling with a negative number) we use the mean absolute values of peak and trough amplitudes discussed in [14]. Distance between individual peaks gives us the separation interval between heart beats and gives us the current heart rate. Figure 5 shows a plot of inter-beat intervals (IBIs) with respect to time and the corresponding frequency domain analysis which is a standard measure of Heart Rate Variability (HRV). Our HRV measure that is visualized (as described below) is the ratio of the normalized low (0.04-0.15Hz) and high (0.15-0.4Hz) frequency powers of the HRV spectrum.

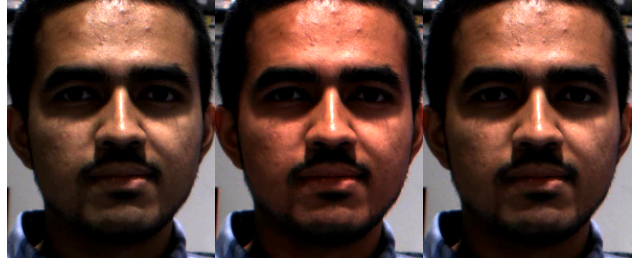


Figure 6. Visualizing the stress level of a subject. Our visualization makes the face color more red with greater HRV low frequency (LF) versus high frequency (HF) power. The HRV LF/HF ratios from right to left are 0.31, 0.62 and 0.48 respectively.

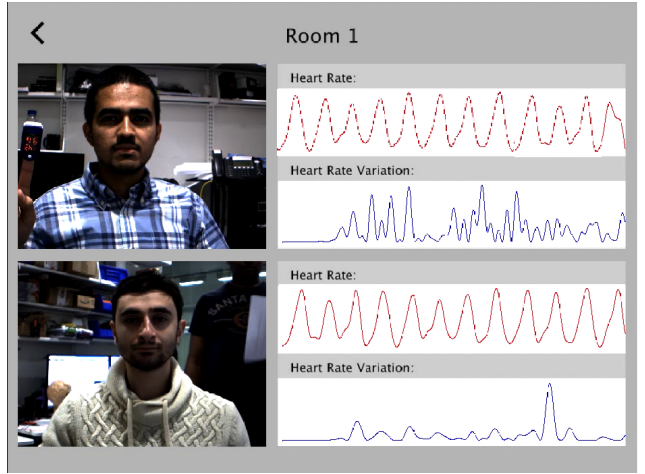


Figure 7. Our system gives accurate readouts of heart rate and HRV LF/HF ratio in real-time. Graphical User Interface (GUI) showing simultaneous measurements for multiple people.

### 3.4. Visualization

Detected HR and HRV can be visualized in multiple ways. For visualizing HRV we change the face color of the subject in real-time. As the low frequency component of their HRV increases in dominance we make the face appear more red (Figure 6). In a separate mode heart rate is visualized by changing the face color at the same frequency as the HR. Please refer to video provided as supplementary material for examples of the visualizations. The visualization can be further extended to a multi-subject setup and can be used to monitor multiple people at the same time using multi-camera arrays (Figure 7) (also see supplementary video). The visualization algorithm uses the facial bounding boxes obtained from the previous steps and applies simple pixel by pixel segmentation in YCbCr space over the ROI to get an accurate mask overlaying face.

## 4. Experiments

Our setup uses a combination of RGB, monochrome and thermal cameras. For the visual spectrum images we used off the shelf cameras: a SONY ICX445 1/3" Global Shutter CCD capable of capturing 1288 x 964 RGB images at 30FPS and a Fujinon YV28x28SA-2 HD Vari-Focal Lens designed for 1/3" sensors. Figure 4 shows the layout of cameras and placement of masks. The cameras are capable of acquiring synchronized video by using external trigger on GPIO pins or internal synchronization over i394 FireWire. For thermal images we use GridEYE sensor connected via I2C to PIC24F04KA200 micro-controller. The 64 2 byte values read from PIC24 are conveyed through FTDI to linux USB. The baseline PPG signal is acquired using an Arduino Pulse Sensor connected to computer through serial over USB. While multi-spectral data acquisition can require very specialized and expensive hardware, we demonstrate how to build this setup with total budget of a few hundred US dollars which can be further reduced to less than \$100 by using cheaper imaging hardware.

### 4.1. Camera Synchronization

For the initial setup, due to bandwidth constraints in our USB 2.0 connection, the cameras were synchronously acquired over the network. We used a TCP handshake to synchronize client-server processes on the machines. We noticed that there could be up to 20 ms of drift for every 30 frames if the acquisition was synchronized every second. Linux kernel modification (reconfiguration of USBFS) allowed us to capture two cameras together on the same machine over USB 3.0. We were able to synchronize the cameras using GPIO triggering but experiments showed that results were fairly accurate without the low level synchronization. GPIO synchronization over the network allows an easy approach for high resolution, high FPS camera arrays and a modest method to circumvent system bus bandwidth issues (since even with 2 cameras raw data readout can be of order of 600Mbps).

### 4.2. Data acquisition

We acquired raw intensity values using the camera SDK and OpenCV. We set the focus and f-stop of the manual lens to get maximum light and good signal. Most modern cameras come with on-board white balance, gain and auto exposure. We also programmed the camera to turn off the auto exposure and white balance algorithms to provide us with the most accurate raw data.

The gold-standard data was acquired by using an FDA approved pulse-oximeter (Drive Medical Design and Manufacturing) and an Arduino Pulse Sensor (for continuous PPG measurement). Subjects were tested at rest and under stress to test accuracy over a range of heart rates. Subjects

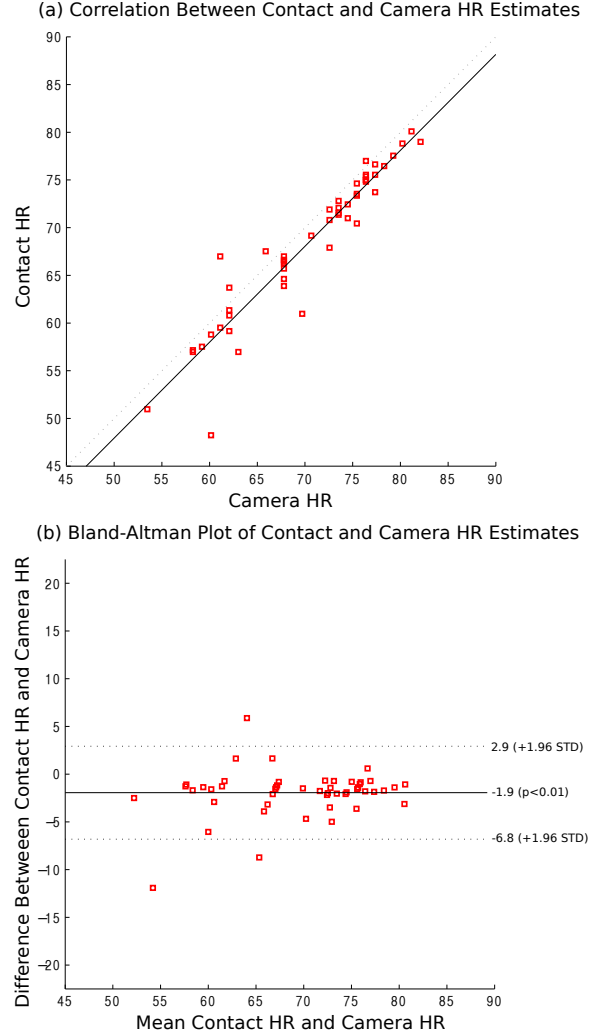


Figure 8. (a) Scatter plot and (b) Bland-Altman plot of the contact and camera measurements for 20 second windows using our multi-camera set-up.

were first recorded for two minutes to give resting heart rate measurements and were later given a mental arithmetic task to induce stress and recorded for a further two minutes. For the validation of our approach we collected data from nine subjects between the ages of 25-40 years. We also made sure to collect data for a wide variation in baseline heart rates and ethnicities (including Caucasian, Asian and South East Asian).

## 5. Results and Discussion

We collected data from the contact PPG sensor in parallel with the thermal sensor, RGB camera and monochrome camera. Two minutes of data were collected for each subject twice and subjects were asked to engage in a mental arithmetic task to induce stress during the second two-

Input Channels vs Heart Rate Measurement Error

<b>GRT</b>	4.62%	<b>BGRM</b>	4.72%
<b>GR</b>	4.77%	<b>GRM</b>	4.86%
<b>GRMT</b>	4.92%	<b>BGR</b>	4.97%
<b>BGRT</b>	5.01%	<b>BGRMT</b>	5.18%
<b>BGMT</b>	5.56%	<b>BGM</b>	5.94%
<b>BGM</b>	5.94%	<b>GM</b>	6.76%
<b>BGT</b>	6.98%	<b>BG</b>	7.42%
<b>BR</b>	7.43%	<b>BRM</b>	7.47%
<b>BRMT</b>	7.80%	<b>GT</b>	8.22%
<b>BMT</b>	8.57%	<b>BM</b>	8.62%
<b>BRT</b>	9.34%	<b>MT</b>	9.49%
<b>BT</b>	10.09%	<b>RM</b>	10.92%
<b>RT</b>	11.65%	<b>RMT</b>	11.68%

Table 2. Measurement error for heart rate estimation within a 20 second window for all combinations of the input channels. R = Red, G = Green, B = Blue, M = Magenta, T = Thermal.

minute period. In order to validate the accuracy of our approach we calculated heart rate estimates from the camera array and the contact sensor within subsequent 20 second windows (no overlap) and compared the measurements.

Figure 8 (a) shows the correlation between the heart rate estimates from our real-time camera set-up and the contact PPG sensor within each 20 second window. Figure 8 (b) shows a Bland-Altman plot of the same data. Table 2 shows the percentage error using all combinations of the possible camera channels. We found a GRT (green, red and thermal) channel combination gave most accurate results (4.62% error) with BGRM and GR coming close second (4.72% and 4.77% error respectively) demonstrating how adding more channels can improve accuracy. As in previous work [14], we observed that simply adding all channels does not provide the best results. There is an optimal selection of frequency filters which can lead to best results and the RGB color channel combination is not optimal (see Table 2). This is explained by the fact that not all spectral channels carry relevant information and adding these channels leads to an increase in signal noise.

Furthermore, we gathered additional data from nine subjects using the camera array and calculated heart rate with or without varying illumination. We observed that using the thermal sensor gave more robust measurements of HR in the presence of illumination changes, as predicted since visible light does not carry long wave infra-red radiation (see Table 3). Our method using a thermal sensor is completely passive and can be used in the dark. This is a considerable improvement over other methods which require the presence of ambient illumination.

Our experiments show how we can use multi-camera arrays in real-time to capture heart rate and heart rate variability. We also demonstrate how to use low cost thermal sensors to capture heart rate in real-time, paving the way

Heart Rate Measurement Error w/ Illumination Variation

<b>Without Illumination Variation</b>	12.63%
<b>With Illumination Variation</b>	9.88%

Table 3. Measurement error for heart rate estimation within a 20 second window for thermal sensor with or without illumination variation.

for capturing heart rate in the absence of illumination. Such a technology could have applications in areas such as night time infant monitoring. We demonstrate how to use the information from the BVP to visualize a person’s stress level in real-time. The user interface we designed can be used to monitor multiple patients in a hospital non-invasively, reducing cognitive overhead of practitioners observing multiple patients overnight. Sudden variations in lighting or absence of lighting can render the conventional camera based heart rate measurement methods useless. However our system is robust under such changes, using thermal sensor to get reliable measurement as shown in Table 3.

## 6. Conclusions and Future Work

We have presented a novel real-time multi-camera system that allows the measurement and visualization of physiological signals. We combine low-cost visual and thermal cameras to create a practical system. We show how we can extend techniques discussed in [14] to use any spectral filter cheaply and effectively. Our multi-camera setup can be used to mimic any color filter array pattern, which otherwise would require expensive equipment and photo-lithography based techniques to fabricate. Furthermore, the addition of a thermal sensor allows for operation under varying ambient illumination. Previous work [14] has shown the advantage of capturing additional color channels for accurate PPG measurement, but used industrial prototypes, limited to the visual range, which are not available commercially.

We have presented a technique to measure heart rate and HRV. HRV is influenced by the autonomic nervous system and lower frequency values for heart rate variability imply higher arousal levels [11]. Our system could be deployed in areas such as hospital patient intake rooms, above the patient bed and in the ICU (and NICU) to monitor the patients’ vital signs non-invasively. We can also use such a camera to monitor health and stress levels for people during daily life and we can design interactive applications to intervene in high stress situations. We have shown that our algorithm is more robust to varying lighting conditions than an RGB camera array. Our method can also be extended to acquire physiological signals of a group of people by running regression forest based facial segmentation for multiple faces and applying ICA on components obtained from the faces. The thermal sensor allows for physiological measurement in the dark, for example when someone is sleeping.



## References

- [1] S. Akselrod, D. Gordon, F. A. Ubel, D. C. Shannon, A. Berger, and R. J. Cohen. Power spectrum analysis of heart rate fluctuation: a quantitative probe of beat-to-beat cardiovascular control. *science*, 213(4504):220–222, 1981. 1
- [2] J. Allen. Photoplethysmography and its application in clinical physiological measurement. *Physiological measurement*, 28(3):R1, 2007. 1
- [3] G. Balakrishnan, F. Durand, and J. Guttag. Detecting pulse from head motions in video. In *Computer Vision and Pattern Recognition (CVPR), 2013 IEEE Conference on*, pages 3430–3437. IEEE, 2013. 3
- [4] N. Blanik, A. K. Abbas, B. Venema, V. Blazek, and S. Leonhardt. Hybrid optical imaging technology for long-term remote monitoring of skin perfusion and temperature behavior. *Journal of biomedical optics*, 19(1):016012–016012, 2014. 2
- [5] F. Bousefsaf, C. Maaoui, and A. Pruski. Remote detection of mental workload changes using cardiac parameters assessed with a low-cost webcam. *Computers in biology and medicine*, 53:154–163, 2014. 2
- [6] M. Dantone, J. Gall, G. Fanelli, and L. V. Gool. Real-time facial feature detection using conditional regression forests. *CVPR*, 13(1):234–778, 2012. 3
- [7] A. Droitcour, V. Lubecke, J. Lin, and O. Boric-Lubecke. A microwave radio for doppler radar sensing of vital signs. In *Microwave Symposium Digest, 2001 IEEE MTT-S International*, volume 1, pages 175–178. IEEE, 2001. 2
- [8] J. R. Estep, E. B. Blackford, and C. M. Meier. Recovering pulse rate during motion artifact with a multi-imager array for non-contact imaging photoplethysmography. In *Systems, Man and Cybernetics (SMC), 2014 IEEE International Conference on*, pages 1462–1469. IEEE, 2014. 2
- [9] M. Garbey, N. Sun, A. Merla, and I. Pavlidis. Contact-free measurement of cardiac pulse based on the analysis of thermal imagery. *Biomedical Engineering, IEEE Transactions on*, 54(8):1418–1426, 2007. 2
- [10] A. Hyvriinen. Fast and robust fixed-point algorithms for independent component analysis. *IEEE Transactions on Neural Networks*, 10(3):626–634, 1999. 4
- [11] D. Kim and Y. Seo. Detection of subjects with higher self-reporting stress scores using heart rate variability patterns during the day. *Biomedical Engineering, IEEE Transactions on*, 49(2):682–685, 2008. 7
- [12] M. Kumar, A. Sabharwal, and A. Veeraraghavan. Robust acquisition of photoplethysmograms using a camera, 2014. 3
- [13] D. McDuff, J. R. Estep, A. M. Piasecki, and E. B. Blackford. A survey of remote optical photoplethysmographic imaging methods. In *Engineering in Medicine and Biology Society (EMBC), 2015 37th Annual International Conference of the IEEE*, pages 6398–6404. IEEE, 2015. 1
- [14] D. McDuff, S. Gontarek, and R. Picard. Improvements in remote physiological measurement using a five band digital camera. *IEEE Transactions on Biomedical Engineering*, 61(9), 2014. 1, 2, 5, 7
- [15] D. McDuff, S. Gontarek, and R. Picard. Remote measurement of cognitive stress via heart rate variability. In *Engineering in Medicine and Biology Society (EMBC), 2014 36th Annual International Conference of the IEEE*, pages 2957–2960. IEEE, 2014. 2
- [16] D. McDuff, J. Hernandez, S. Gontarek, and R. W. Picard. Cogcam: Contact-free measurement of cognitive stress during computer tasks with a digital camera. In *Proceedings of the SIGCHI Conference on Human Factors in Computing Systems*. ACM, 2016. 2
- [17] M.-Z. Poh, D. McDuff, and R. W. Picard. Non-contact, automated cardiac pulse measurements using video imaging and blind source separation. *Optics Express*, 18(10):10762–10774, 2010. 1, 2, 5
- [18] M.-Z. Poh, D. McDuff, and R. W. Picard. Advancements in noncontact, multiparameter physiological measurements using a webcam. *Biomedical Engineering, IEEE Transactions on*, 58(1):7–11, 2011. 1, 2
- [19] Y. Sun, S. Hu, V. Azorin-Peris, S. Greenwald, J. Chambers, and Y. Zhu. Motion-compensated noncontact imaging photoplethysmography to monitor cardiorespiratory status during exercise. *Journal of Biomedical Optics*, 16(7):077010–077010, 2011. 3
- [20] L. Tarassenko, M. Villarroel, A. Guazzi, J. Jorge, D. Clifton, and C. Pugh. Non-contact video-based vital sign monitoring using ambient light and auto-regressive models. *Physiological measurement*, 35(5):807, 2014. 1, 3
- [21] M. P. Tarvainen, P. O. Ranta-aho, and P. A. Karjalainen. An advanced detrending method with application to hrv analysis. *Biomedical Engineering, IEEE Transactions on*, 49(2):172–175, 2002. 3
- [22] S. S. Ulyanov and V. V. Tuchin. Pulse-wave monitoring by means of focused laser beams scattered by skin surface and membranes. In *OE/LASE'93: Optics, Electro-Optics, & Laser Applications in Science & Engineering*, pages 160–167. International Society for Optics and Photonics, 1993. 2
- [23] W. Verkruijsse, L. O. Svaasand, and J. S. Nelson. Remote plethysmographic imaging using ambient light. *Optics express*, 16(26):21434–21445, 2008. 1, 2
- [24] H.-Y. Wu, M. Rubinstein, E. Shih, J. Guttag, F. Durand, and W. Freeman. Eulerian video magnification for revealing subtle changes in the world. *ACM Transactions on Graphics (TOG)*, 31(4):65, 2012. 3